Journal of Advances in Science and Technology

Vol. X, Issue No. XX, November-2015, ISSN 2230-9659

AN ANALYSIS UPON DIFFERENT CHARACTERIZATION TECHNIQUES FOR THE CATALYSTS PREPARATION

AN INTERNATIONALLY INDEXED PEER REVIEWED & REFEREED JOURNAL

www.ignited.in

Journal of Advances in Science and Technology
Vol. X, Issue No. XX, November-2015, ISSN 2230-9659

An Analysis upon Different Characterization Techniques for the Catalysts Preparation

Sandeep Kumar[1]* Dr. Sanjay Chaudhary[2]

[1] Research Scholar, Maharishi University of Information Technology, Lucknow

[2] Professor, Maharishi University of Information Technology, Lucknow

Abstract – Describes the physical properties of the catalysts obtained on the basis of the characterization techniques. The cation exchange capacity (CEC) of fly ash was enhanced after acid/alkali treatment and metal impregnation and this has been attributed to creation of defect sites and broken bonds on the oxide surfaces. Overall the order of increasing CEC is as follows:

F2 > N2 > C2 > M2 > F1 >N1 > C1 > M1 > F3 > C3 > N1 > M3 >> O

AAS measurements showed that the amount of Fe(III), Co(II), Ni(II) and Mn(II) entering into the fly ash material was different and follow the order of: Fe(III) > Co(II) > Ni(II) > Mn(II). XRF results confirm that silica is the major oxide and all the fly ash catalysts belong to Class F type fly ash. The LOI value (w/w %) also increased after metal impregnation.

The XRD spectra could show the differences in crystallinity and other properties in terms of the changes in the diffraction bands of the fly ash catalysts before and after acid/alkali or metal impregnation treatment. These results were supplemented with the FT–IR study. It was observed that the M–O stretching band shifted after acid and alkali treatment of the fly ash for all the eight catalysts. However, formation of new bonds was not observed in any of the cases, indicating little change in chemical properties of the metal oxides.

Scanning electron micrographs showed that the surfaces became rough and more porous after treatment of the fly ash with acid and alkali. After metal impregnation, the grains of salts over the surface of fly ash are clearly visible. BET adsorption-desorption isotherms of raw fly ash and the metal impregnated catalysts yielded Type II nitrogen adsorption isotherm with H3 hysteresis loop. The measurements indicated that both surface area and pore volume are higher for the acid treated fly ash catalysts than the others (water washed and alkali treated fly ash based catalysts) and the maximum surface area was found in acid treated Fe(III)-catalyst (F2) (3.60 m^2/g).

----------♦----------

INTRODUCTION

This chapter describes the results of different characterization techniques for the catalysts prepared in this work. The impregnated Fe(III)-, Co(II)-, Ni(II)- and Mn(II)-fly ash and their acid and alkali treated forms were characterized with cation exchange capacity (CEC) measurement, atomic absorption spectrometry (AAS), X-ray diffraction (XRD), X-ray fluorescence (XRF), Fourier transform infrared spectrophotometry (FTIR), scanning electron microscopy (SEM), BET surface area and pore size determination.

CATION EXCHANGE CAPACITY (CEC)

The cation exchange capacities (CEC) of the materials, determined with copper bisethylenediamine complex method (Bergaya and Vayer, 1997) are given below.

Materials-		CEC (meq/kg)
O`	Uncalcined fly ash	15.5
O	Calcined water-washed fly ash	22.6
A	Acid treated fly ash	32.7
B	Alkali treated fly ash	30.2
M1	Mn(II)-water-washed fly ash	48.7
M2	Mn(II)-acid treated fly ash	63.7
M3	Mn(II)-alkali treated fly ash	37.5
C1	Co(II)-water-washed fly ash	51.7
C2	Co(II)-acid treated fly ash	66.2
C3	Co(II)-alkali treated fly ash	41.2
N1	Ni(II)-water-washed fly ash	56.7
N2	Ni(II)-acid treated fly ash	71.3
N3	Ni(II)-alkali treated fly ash	40.1
F1	Fe(III)-water-washed fly ash	58.1
F2	Fe(III)-acid treated fly ash	86.5
F3	Fe(III)-alkali treated fly ash	43.6

It is observed that in all the cases, the cation exchange capacity increases after treatment (either acid or alkali). However it is observed that the effect is more in the acid treated fly ash. Of all the metal incorporated fly ash, Fe(III)-acid treated fly ash has the highest CEC that has increased by ~ 2.6 times of the CEC of the acid-treated fly ash (with 1.0 M H_2SO_4) without Fe(III) incorporation.

Koukouzas et al. (2010) have reported that the CEC of coal fly ash was 1.4 to 17.4 meq/kg. Another group of workers, Izidoro et al. (2012) have also found the CEC of Brazilian coal ash as 35.0 meq/kg. These values are much lower than the values obtained in the present work. In earlier work, Woolard et al. (2000) had reported that on hydrothermal treatment of coal fly ash with NaOH, the CEC of the material was increases. This result was supported by Singer et al. (1995). They had reported that on treatment of coal FA (20 g) with 3.5 N NaOH (160 ml) for 6h, the cation exchange capacity was tremendously increased and showed > 2.5 to 3.0 meq/g. in the present work, the cation exchange capacity of the alkali treated FA was higher than raw FA (O), which is in agreement with the result obtained by Woolard et al. (2000) and Singer et al. (1995). But the rate of increases was not same in the present case. This might be due to the strength of the NaOH (1.0 M) which is much lower than that used by Woolard et al. (2000) and Singer et al. (1995).

According to Chaliha et al. (2008), the CEC of a material increases due to the increase in the number of cation exchangeable sites. Thus, it may be inferred that in the present case, after acid or alkali or metal impregnation processes, the number of such exchangeable sites increases. Rodrigues et al. (2003) have suggested that the increase in the exchangeable sites of a material might be due to the creation of defect sites and broken bonds present on the surface of the materials.

MEASURING FE(III)-, CO(II)-, NI(II)- AND MN(II) IN THE CATALYSTS (BY AAS)

The amount of Fe(III), Co(II), Ni(II) and Mn(II) entering into the fly ash material was determined with atomic absorption spectrometric measurement. The amounts of Fe, Co, Ni and Mn in the calcined raw fly ash and metal impregnated fly ash catalysts are given in Table 1.

From the results of AAS analysis, the following inferences can be made:

a) The parent fly ash material (calcined) contained the four metals in the order of Fe(III) > Ni(II) > Mn(II) > Co(II).

b) The contents changed drastically after incorporation of a transition metal cation by refluxing with a solution of a particular metal salt for 6 h at 373 K – the content of that particular metal increased (indicating metal incorporation) while there was huge loss in the other three metals. Thus, when Mn(II) was incorporated into

(i) the water-washed fly ash, the contents of Co(II), Ni(II) and Fe(III) came down from 7.48 to 0.26 mg/kg, 17.89 to 0.23 mg/kg, and 83.90 to 17.80 mg/kg respectively;

(ii) the acid-treated fly ash, the contents of Co(II), Ni(II) and Fe(III) came down from 7.48 to 0.18 mg/kg, 17.89 to 0.26 mg/kg, and 83.90 to 25.40 mg/kg respectively;

(iii) the alkali-treated fly ash, the contents of Co(II), Ni(II) and Fe(III) came down from 7.48 to 0.28 mg/kg, 17.89 to 0.40 mg/kg, and 83.90 to 17.31.40 mg/kg respectively;

Very similar results were observed during incorporation of the transition metal cations, Co(II), Ni(II) and Fe(III) into acid-washed and alkali-washed fly ash. The huge loss of the metal cations when one particular cation was introduced by refluxing at 373 K for 6 h is obviously due to replacement of the existing metal cation by the one being incorporated and also due to leaching at the higher temperature.

c) Although metal incorporation was done by taking the same strength of the metal solution (i.e. 1 molar solution), different amounts of Mn(II), Co(II), Ni(II) and Fe(III) entered into acid and alkali treated fly ash. The calcined raw fly ash contained 0.013 % Mn(II), which increased to 0.045 % in water-washed fly ash, 0.022 % in acid-treated fly ash and 0.028 % in alkali-treated fly ash. This indicated that maximum Mn(II) incorporation was possible in case of water- washed fly ash and that the alkali-treated fly ash could take up a little more of Mn(II) than the acid-treated fly ash.

Table 1: Mn(II), Co(II), Ni(II) and Fe(III) in the calcined raw fly ash (FA) and water-washed, acid- and alkali-treated catalysts

Material	Mn(II)		Co(II)		Ni(II)		Fe(III)	
	mg/kg	%	mg/ kg	%	mg/ kg	%	mg/ kg	%
FA	12.52	0.013	7.48	0.0075	17.89	0.018	83.90	0.084
M1	45.05	0.045	0.26		0.23		17.80	0.018
M2	21.61	0.022	0.18		0.26		25.40	0.025
M3	27.65	0.028	0.28		0.40		31.40	0.031
C1	0.32		60.89	0.061	0.09		24.60	0.025
C2	0.35		97.48	0.097	0.08		65.60	0.066
C3	0.39		54.83	0.055	0.12		54.10	0.054
N1	0.53		0.10		70.46	0.070	50.60	0.051
N2	0.30		0.08		66.48	0.066	29.38	0.029
N3	0.38		0.08		58.70	0.059	29.38	0.029
F1	0.38		0.09		0.12		134.80	0.135
F2	0.43		0.77		0.13		165.50	0.166
F3	0.45		0.27		0.33		154.67	0.155

d) The calcined raw fly ash already contained 0.0075 % Co(II). On impregnation, Co(II) increased to 0.061 % in water-washed fly ash, 0.097 % in acid-treated fly ash and 0.055 % in alkali-treated fly ash. Maximum Co(II) impregnation was possible in case of acid-treated fly ash. The water washed and the alkali-treated fly ash could take up a little less Co(II) than the acid-treated fly ash.

e) When impregnating the fly ash with Ni(II), the content increased from 0.018 % (the amount in the calcined raw fly ash) to 0.070 % in water-washed fly ash, to 0.066 % in acid-treated fly ash and to 0.059 % in alkali-treated fly ash. It was observed that the maximum amount of Ni(II) incorporation was possible in case of water-washed fly ash followed by the acid-treated fly ash and the alkali-treated fly ash.

f) The calcined raw fly ash contained 0.084 % Fe(III) which increased to 0.135 % in water-washed fly ash, 0.166 % in acid-treated fly ash and 0.155 % in alkali-treated fly ash. This indicated that maximum Fe(III) incorporation was possible in case of water-washed fly ash and that the alkali-treated fly ash could take up a little more of Fe(III) than the acid-treated fly ash.

XRF MEASUREMENTS

X-ray fluorescence (XRF) measurement is one of the preferred methods for the determination of the principal components present in a material. The coal fly ash sample and its metal impregnated forms were subjected to X-ray fluorescence (XRF) analysis using Philips PW 1480 (Rh anode and LiF 200 crystal analyzer) spectrometer. The chemical composition of the coal fly ash with respect to the major oxides (% w/w) obtained from XRF is given in Table 2.

Table 2 shows that the major components of the fly ash, used in this work, are silica (SiO_2), alumina (Al_2O_3), ferrous oxide (Fe_2O_3), and sodium oxide (Na_2O) with varying amounts of unburnt carbon as measured by the Loss on Ignition (LOI).

From the results, the following conclusions may be made about the composition of the fly ash samples:

(i) The principal oxides were present in the order of SiO_2 >> Al_2O_3 >> Fe_2O_3 > Na_2O ≈ K_2O ≈ CaO ≈ TiO_2 > P_2O_5 >> MnO ≈ MgO in the coal fly ash. Such observations have also been made earlier (Dutta et al., 2009; Sahu et al., 2009; Mishra et al., 2010; Blissett et al., 2012)

(ii) The chemical composition is dominated by silica constituting more than 50 % (by wt) of the total composition of the materials.

(iii) In all the metal impregnated fly ash materials, the oxide composition is in similar order, but with much less of Al_2O_3 compared to the parent fly ash indicating loss of Al(III) during the treatments. It is also observed that al the metal impregnated fly ash materials contained less K_2O, CaO, TiO_2 and P_2O_5 compared to the parent fly ash. The alkali-treated fly ash has also shown a large Al_2O_3 loss comparable to those of the transition metal-incorporated fly ash catalysts. Al_2O_3 loss during alkali treatment may be explained by dissolution of a large amount of the oxide forming soluble Na-aluminate. The loss during transition metal cation incorporation might be due to refluxing of the material with an appropriate salt solution for 6 h at 373 K, which led to almost equal loss of Al_2O_3 in all the materials.

(iv) The American Society for Testing and Materials (ASTMs) has broadly classified the fly ash materials into two chemical types according to their industrial application– Class F and Class C. In the Class F type, the composition has SiO_2 + Al_2O_3 + Fe_2O_3 ≥ 70 % whereas the second type has the sum of the three oxides in the range of 50 – 70 % (Manz, 1999; Vassilev et al., 2007; Wang, 2008; Mavrikos et al., 2014). In the present work, it is observed that silica, alumina and iron oxide are the three main constituents of fly ash and they together make up 60 - 70 % by wt in the alkali-treated fly ash and all the metal incorporated fly ash catalysts. These materials in this study may be considered as belonging to Class C as per ASTM classification. The parent uncalcined fly ash (O`), the calcined fly ash (O) and the acid-treated fly ash (A) are made up of more than 70 % (by wt) of the three major oxides, and therefore these belong to Class F materials.

Table 2. Chemical Composition (wt %) of the uncalcined and calcined samples of the raw fly ash (O` and O), the acid and alkali treated fly ash (A and B) and all the twelve metal impregnated fly ash (M1, M2, M3, C1, C2, C3, N1, N2, N3, F1, F2, F3)

Sample	SiO_2	Al_2O_3	Fe_2O_3	MnO	MgO	CaO
O`	57.98	21.81	5.40	0.050	0.88	1.59
O	56.81	21.37	5.00	0.040	0.31	1.34
A	58.80	21.77	5.19	0.050	0.19	1.21
B	58.49	12.21	3.34	0.190	0.06	1.16
M1	55.96	12.07	3.89	0.219	0.06	1.36
M2	52.54	13.21	2.86	0.218	0.21	0.37
M3	54.78	13.98	3.21	0.189	0.10	0.69
C1	48.84	11.31	2.67	0.016	0.69	0.59
C2	55.51	11.38	1.83	0.008	0.08	0.13
C3	54.86	11.39	2.01	0.007	0.09	0.15
N1	51.44	11.77	2.11	0.009	0.06	0.46
N2	51.28	11.58	1.68	0.006	0.07	0.09
N3	51.54	11.49	2.18	0.007	0.08	0.36
F1	58.99	14.51	6.80	0.035	0.12	0.61
F2	56.27	13.12	9.71	0.014	0.10	0.21
F3	55.12	11.39	8.95	0.066	0.14	0.57

Sample	Na_2O	K_2O	TiO_2	P_2O_5	LOI
O`	3.14	2.83	2.15	1.310	2.76
O	2.19	2.07	1.91	1.220	7.74
A	2.21	2.89	1.82	1.120	4.94
B	2.17	0.96	1.01	0.091	20.32
M1	2.16	1.19	1.16	0.087	22.03
M2	2.18	1.13	0.86	0.052	26.37
M3	2.17	0.82	0.92	0.095	23.05
C1	2.16	0.72	0.75	0.118	32.14
C2	2.17	0.86	0.54	0.023	27.47
C3	2.16	0.76	0.71	0.103	27.76
N1	2.16	0.61	0.63	0.091	30.66
N2	2.17	0.78	0.53	0.022	31.79
N3	2.16	0.68	0.61	0.067	30.83
F1	2.17	1.25	1.25	0.109	14.16
F2	2.18	1.26	0.84	0.035	16.26
F3	2.16	1.21	1.09	0.055	19.25

(v) Loss on ignition (LOI), determined by heating up to 950^{o}C, shows that compared to the original fly ash, the alkali-treated fly ash and all the impregnated fly ash samples had higher LOI indicating the presence of large amounts of volatile matter.

The relative amounts of the oxides agreed well with those reported earlier (Jime´nez et al., 2003; Sarkar et al., 2006, Mishra et al., 2010). The composition of the raw uncalcined fly ash in the present work is similar to that of the common bituminous coal fly ash, defined as class F by American Society for Testing Materials (ASTM, 2005; Ahmaruzzaman, 2010). Banerjee et al. (2003) had reported that the loss of ignition of fly ash and the Al^{3+} and Fe^{3+}-impregnated fly ash is ~ 13 % in their study in the removal of transition metals from wastewater by adsorption with the help of FA. Bayuseno et al. (2011) had reported that the LOI for municipal solid waste incinerator (MSWI) FA (< 100 µm particle size) was about 8.5 wt.% when the material is heated for about 750 ^{0}C which is in agreement with the result obtained by Quina et al. (2008). According to them, the loss of ignition was due to the high concentration of unburned carbon. Remond et al. (2002) had reported the same in the range of 2 to 5 %, due to the releases of CO_2 and HCl from the decomposition of $CaCO_3$ and CaOHCl. Singh et al. (2015) had reported that with decrease in parcel size of the fly ash material, the LOI also decreases. They had observed that as the particle size of FA decreased from 150 µm to 45 µm, the LOI at 800 ^{0}C decreased from 12.0 to 4.1 wt %.

XRD ANALYSIS OF THE FLY ASH SAMPLES

Powder X-ray diffraction (PXRD) patterns of the fly ash samples were taken using Pan Analytical X-Ray Spectrophotometer, PW 1710, Cu Kα radiation (Sophisticated Instruments Facility, Gauhati University).

The uncalcined raw fly ash (O`) yielded 6 bands in the range of 1 – 30^{o} (2θ), the major band appearing at 2θ = 26.61^{o} (d = 3.35 Å). After calcination, the raw fly ash gave three XRD bands at d = 5.36, 4.25 and 3.35 Å having the same major peak as that of uncalcined one (Fig 1). These results are in conformity with the known XRD pattern of coal fly ash (Jime´nez et al., 2003; Sarkar et al., 2006; Li et al., 2009; Johnson et al., 2010; Reinika et al., 2011). The most prominent XRD band in all the catalysts was observed at the same 2θ range of ~ 26.5 to 26.7. These values correspond to quartz indicating silica to be a major constituent of the fly ash. The XRD bands and their characteristics are shown in Table 3.

Table 3. 2θ and d spacings of the different crystallographic planes of uncalcined and calcined raw fly ash (O`and O)

O`			O		
Angle (2θ) (deg)	Relative intensity (%)	d-spacing (Å)	Angle (2θ) (deg)	Relative intensity (%)	d-spacing (Å)
9.67	50.67	2.42	16.54	4.31	5.36
26.61	100	3.35	20.88	13.39	4.25
28.65	67.8	3.12	26.65	100.00	3.30

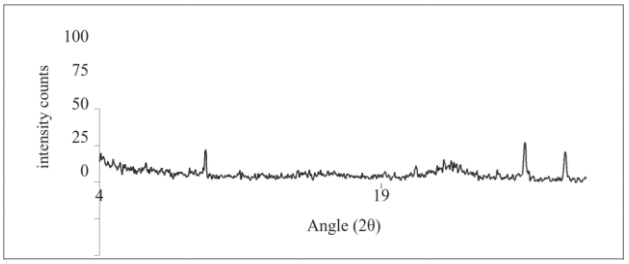

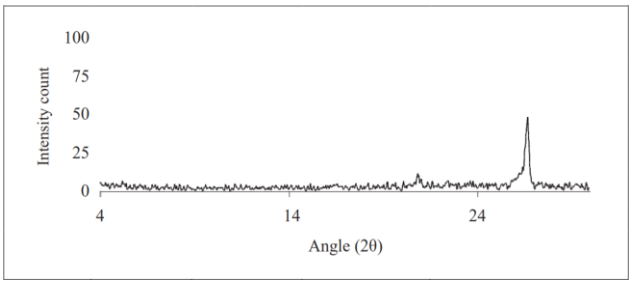

Figure. 1. XRD patterns of uncalcined (top) and calcined raw fly ash (bottom).

It can be inferred from the XRD data that all the fly ash materials had similar X-ray diffraction patterns indicating similarity in their mineralogical composition. The X-ray diffractograms of all the metal impregnated fly ash samples are given in Figs. 2, 3, 4 and 5. Another mineral, mullite, was also found in the fly ash samples indicated by strong peaks at 2θ = 28.65^{o} (d: 3.12) for the uncalcined fly ash material. Similar results have been reported for a fly ash sample by Jason et al., 2005; Vermaak et al., 2008;, Kishore et al., 2002; Yaumi et al., 2013; Sharma et al. (2013) which show that quartz, mullite, iron oxide are the major components in the fly ash.

The intensity of quartz XRD peak was very strong in each of the fly ash samples, with mullite as another chemically stable component, which was, however, not observed in all the samples.

Sarkar et al. (2006) observed that the increase in quartz content leads to decrease in particle size distribution of fly ash. Bhargava et al. (1993) also observed that the acid treatment of fly ash will induce surface changes and influence the degree of adsorption of the adsorbates onto the fly ash surface. The XRD patterns of the fly ash material reveal that the uncalcined fly ash is a largely amorphous glassy material.

Since the raw fly ash after calcination did not show any remarkable differences in their XRD patterns, it is clear that calcination did not alter the chemical phases present in the raw fly ash. However, it was observed that after calcination, the intensity of the main quartz XRD peak was enhanced which indicate the enhancement of crystallinity in the fly ash material due to calcination.

The results of powder X-ray diffraction measurements of the metal impregnated fly ash catalyst are discussed below.

Mn(II) impregnated fly ash-

In this work, Mn(II) impregnated fly ash shows (Fig. 2) a strong basal peak at ~26.5 to 26.8 which is typical for quartz indicating the main constituent of the material to be quartz. The XRD bands and their characteristics are shown in Table 4. The water washed Mn(II) impregnated fly ash (M1) had major XRD bands at 8.88, 17.8, 20.92, 26.69^{0} (2θ) corresponding to d spacings of 9.95, 4.98, 4.24, 3.33 Å respectively. In the acid treated Mn(II) impregnated fly ash (M2), the 2θ value shifts towards the lower angles accompanied by increase in intensities of the bands (17.79, 20.87^{0} (2θ)). In addition to that the band obsrved at 8.88^{0} (2θ) in M1 vanishes and a new XRD band at 27.79^{0} (2θ) corresponding to d spacing of 3.21 Å appaers. This band might be due to the mineral mullite which was also observed in the parent fly ash material (O`) at 28.65^{0} (2θ). In the alkali treated Mn(II) impregnated fly ash (M3), the bands shift towards lower angles (16.27, 20.7, 26.51^{0}) and the intensities of the bands decrease. It has to be mentioned that the band obsrved at 8.88^{0} (2θ) in M1 shifted to 9.48^{0} (2θ) in M3 corresponding to d spacing of 9.32 Å. 2θ and d values for all the three Mn(II) impregnated catalysts are given in Table 4.

XRD patterns of the Mn(II) impregnated samples (M1, M2, M3) indicated no remarkable differences in the XRD patterns. Therefore, the treatment with either alkali or acid or Mn(II) transition metal salt solutions did not alter the chemical phases present in the raw fly ash material. However, it was observed that treatment with acid and alkali effects the intensities of the main quartz XRD peak. In the case of acid treated Mn(II) impregnated fly ash (M2), the intensity of the characteristic basal peak of quartz (26.6^{0}) was successively increased and for the alkali treated Mn(II) impregnated fly ash, the intensity of the quartz peak (26.51^{0}) decreased compared to that of the raw fly ash (O). This implies that after alkali treatment, the crystallinity of the fly ash decreases. According to Bada et al (2008) in the study of adsorption capacity of Southern African coal fly ash had reported that due to the acid treatment over the FA material, corrosion of the outer glassy layers i.e., chains of Si, Al and Ca takes place that lead to the increase in intensity of the quartz peak. They reported that due to the acid treatment, the particle distribution of FA decreases that affect the surface property of the FA material. This result was supported by both Sarkar et al. 2006 and Bhargava et al (1993).

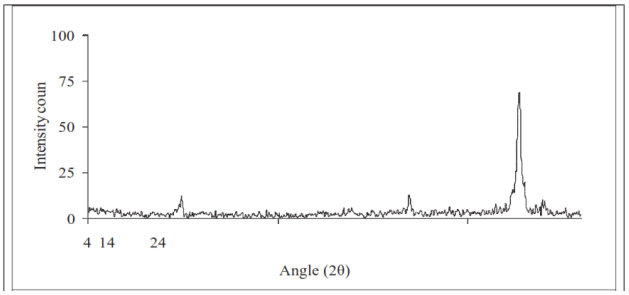

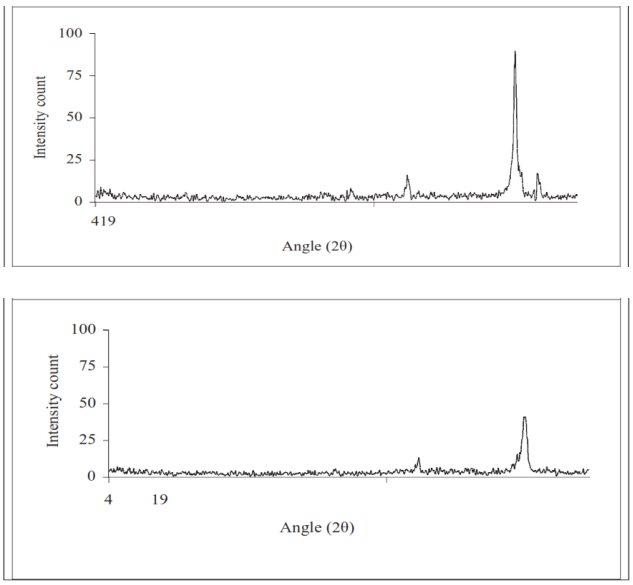

Figure. 2. XRD patterns for calcined Mn(II)-impregnated water washed (M1, top), acid treated (M2, middle) and alkali treated (M3, bottom) fly ash catalysts.

Table 4. 2θ and d spacings of the different crystallographic planes of Mn(II)- impregnated fly ash (calcined water washed FA in M1, acid-treated FA in M2, alkali treated FA in M3)

M1			M2			M3		
Angle (2θ) (deg)	Relative intensity (%)	d-spacing (Å)	Angle (2θ) (deg)	Relative intensity (%)	d-spacing (Å)	Angle (2θ) (deg)	Relative intensity (%)	d-spacing (Å)
8.88	11.01	9.95	17.79	5.53	4.98	9.48	2.67	9.32
17.80	3.61	4.98	20.87	9.62	4.25	16.27	7.09	5.44
20.92	13.87	4.24	26.60	100.00	3.35	20.7	21.88	4.29
26.69	100.00	3.33	27.79	13.11	3.21	26.51	100.00	3.36

Co(II) impregnated fly ash-

Co(II) impregnated fly ash viz. C1, C2, C3 showed (Fig.3) a strong basal peak at ~26.5 to 26.6 which is typical for quartz indicating that the main constituent of the Co(II) impregnated fly ash is quartz. The XRD bands and their characteristics are shown in Table 5. The water washed Co(II) impregnated fly ash (C1) had major XRD bands at 16.33, 20.68, 26.53^0 (2θ) corresponding to d spacings of 5.42, 4.29, 3.35 Å respectively. In the acid treated Co(II) impregnated fly ash (C2), the 2θ value shifts towards higher angles, accompanied by an increase in intensities of the bands, in particular, that of the 26.59^0 (2θ) band. An additional band at about 27.92^0 (2θ) with relative intensity of 8.23 % and d spacing of 3.19 Å was also observed. This band was absent in the water washed Co(II) impregnated fly ash. This band might be due to the presence of mullite in the fly ash material. However, in the case of alkali treated fly ash material (C3), only two bands were observed. A stong band at ~ 26.56^0 (2θ) and d spacing of 3.36 Å and a weak band at around 20.67^0 and d spacing of 4.27 Å respectively could also be assigned to quatz. The 2θ and d values for all the three Co(II) impregnated catalysts along with their relative intensities (%) are given in Table 5.

Table 5. 2θ and d spacings of the different crystallographic planes of calcined water washed, acid and alkali treated Co(II)- impregnated fly ash (C1, C2 and C3).

C1			C2			C3		
Angle (2θ) (deg)	Relative intensity (%)	d-spacing (Å)	Angle (2θ) (deg)	Relative intensity (%)	d-spacing (Å)	Angle (2θ) (deg)	Relative intensity (%)	d-spacing (Å)
16.33	6.71	5.42	17.64	2.32	5.02	20.79	6.52	4.27
20.68	16.92	4.29	20.84	10.92	4.26	26.56	100.00	3.36
26.53	100.00	3.35	26.59	100.00	3.35			
			27.92	**8.23**	**3.19**			

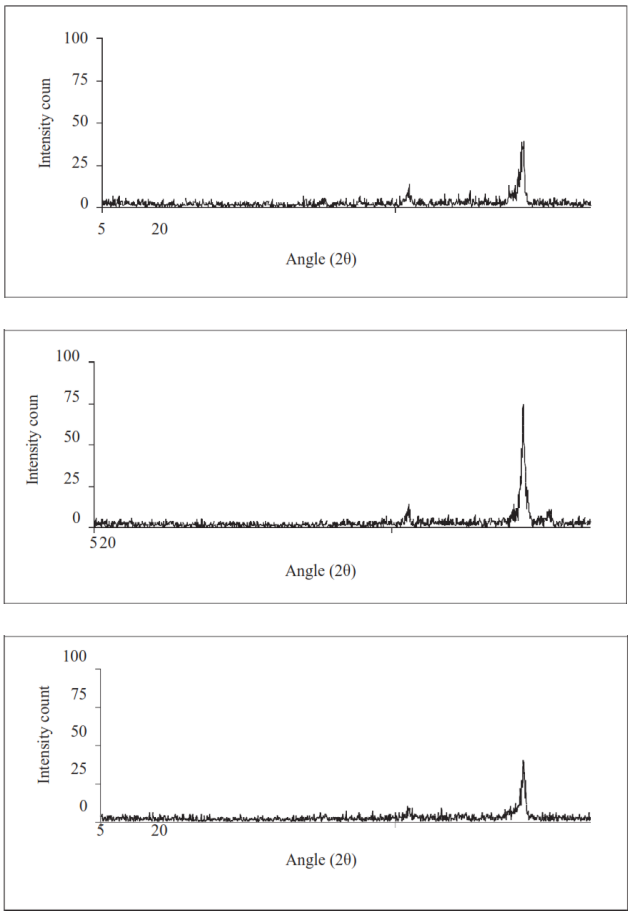

Figure. 3. XRD patterns of calcined Co(II)-impregnated water washed (C1, top), acid treated (C2, middle) and alkali treated (C3, bottom) fly ash catalysts.

The XRD patterns of all the three Co(II) impregnated materials (C1, C2, C3), also show that there was no change in the chemical phases present in the fly ash following the treatments and Co(II) impregnation. The major basal peak was for quartz in the range of 26.5 to 26.6^0 (2θ) with d-spacing of ~ 3.35 Å. Small shifts in the quartz band and considerable changes in the band intensities were, however, observed. In the acid treated Co(II) impregnated fly ash (C2), the intensity and the diffraction angle (2θ) of the characteristic basal peak of quartz (26.59^0) were higher compared to the water washed fly ash, whereas for the alkali treated Co(II) fly ash (C3), the intensity and 2θ of the quartz peak (26.56^0) were very similar to those of C1. Acid treatment must have removed some of the

amorphous material at the surface increasing X-ray penetration and improving the intensity of the diffracted beam.

Ni(II) impregnated fly ash-

The XRD bands of Ni(II) impregnated fly ash (N1, N2, N3) were shown in Fig. 4 which showed that all the three catalysts had a strong basal peak at ~26.4 to 26.7 typical for quartz. The bands did not show any significant shift when compared to the un- impregnated fly ash. All the XRD bands and the characteristics of the three catalysts are shown in Table 6.

Table 6. 2θ and d spacings of the different crystallographic planes of calcined water washed, acid and alkali treated Ni(II)- impregnated fly ash (N1, N2 and N3)

N1			N2			N3		
Angle (2θ) (deg)	Relative intensity (%)	d-spacing (Á)	Angle (2θ) (deg)	Relative intensity (%)	d-spacing (Á)	Angle (2θ) (deg)	Relative intensity (%)	d-spacing (Á)
26.42	100.00	3.37	8.87	7.31	9.96	16.64	8.13	5.32
			20.86	21.14	4.25	21.01	9.03	4.22
			26.63	100.00	3.34	26.68	100.00	3.31
			27.98	4.32	3.19			

The water washed Ni(II) impregnated fly ash (N1) showed only one major XRD band at 26.42^0 (2θ) corresponding to d spacings of 3.37 Á. After Ni(II) impregnation, the angle of diffraction (2θ) corresponding to quartz shifted towards lower angles accompanied by decrease in intensitiy as well as the d-spacing. However, in the acid treated Ni(II) impregnated fly ash (N2), the major XRD bands were at 8.87, 20.86, 26.63, 26.98^0 (2θ) corresponding to d spacings of 9.96, 4.25, 3.34, 3.19 Á respectively. In this case, no significant change was observed compared to the original fly ash (O` and O). similler to this result, the alkali treated fly ash (N3) did not show much changes in their XRD bands implying that after metal impregnation, the alkali and acid treated fly ash materials did not alter the chemical phases present in the raw fly ash (O`/ O).

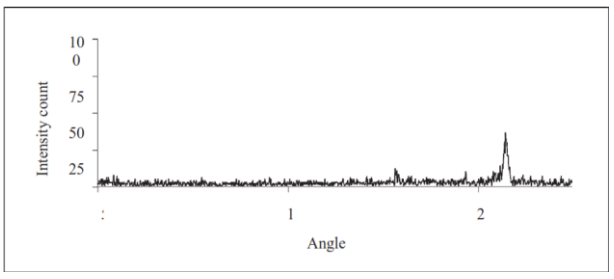

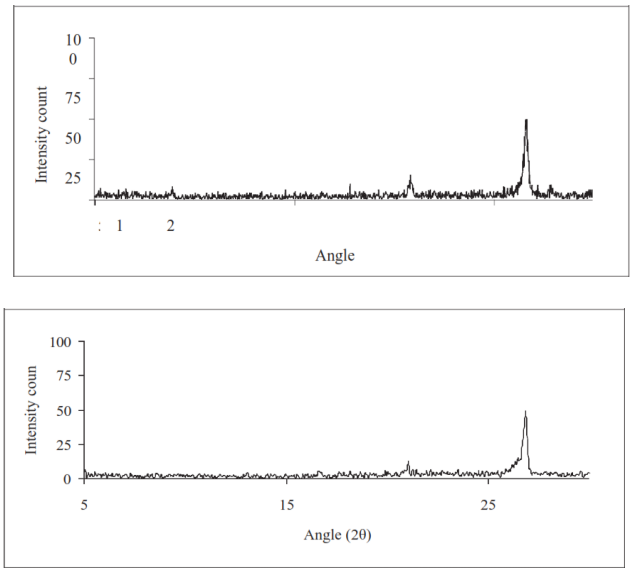

Figure. 4. XRD patterns for calcined Ni(II)- impregnated water washed (N1, top), acid treated (N2, middle) and alkali treated (N3, bottom) fly ash catalysts.

Fe(III) impregnated fly ash-

Fe(III) impregnated fly ash (F1, F2, F3) also showed (Fig. 4) a strong basal peak at ~26.6 to 26.7 due to the presence of quartz as a major constituent. The XRD data of all the three Fe(II) impregnated fly ash materials are shown in Table 7.

In the water washed Fe(III) impregnated fly ash (F1), five major XRD bands were observed at 8.73, 11.94, 20.16, 24.74 and 26.69^0 (2θ) corresponding to d spacings of 10.13, 7.41, 4.40, 3.59, 3.35 Á respectively. These bands are similar to thise in the raw fly ash material.

Table.7. 2θ and d spacings of the different crystallographic planes of calcined water washed, acid and alkali treated Fe(II)- impregnated fly ash (F1, F2 and F3)

F1			F2			F3		
Angle (2θ) (deg)	Relative intensity (%)	d-spacing (Á)	Angle (2θ) (deg)	Relative intensity (%)	d-spacing (Á)	Angle (2θ) (deg)	Relative intensity (%)	d-spacing (Á)
8.73	20.77	10.13	8.89	7.05	9.94	20.7	6.71	4.29
11.94	7.65	7.41	17.87	5.65	4.96	26.56	100.00	3.36
20.16	12.58	4.40	20.89	17.5	4.25			
24.74	20.68	3.59	26.66	100.00	3.34			
26.59	100.00	3.35	26.95	52.42	3.31			

However a new band at 24.74^0 (2θ) with d-spacing of 3.59 Á, likely to be due the presence of mullite, was observed. In the acid treated Fe(III) impregnated fly ash (F2), similar bands were observed with 2θ shifting a little towards higher angle, accompanied by increase in intensities of the bands (8.89, 17.87, 20.89, 26.66, 26.95^0 (2θ)) and also the d-spacing. Contrary to this, the alkali treated Fe(III) impregnated

fly ash showed only two major peaks at 20.70 and 26.56^0 (2θ) corresponding to d spacings of 4.29 and

3.35 Å respectively, which were also due to quartz

As in the other cases, the XRD patterns of the Fe(III) impregnated samples (F1, F2, F3), did not show any remarkable difference with the raw fly ash material. Therefore, it is clear that the treatment with either alkali or acid or Fe(III) transition metal salt solution did not alter the chemical phases present in the raw fly ash material. However, it was observed that after metal impregnation the intensities of the main quartz XRD peak changes a little in all the three catalysts.

Khatri et al., (2008) had reported that after activation of fly ash with concentrated H_2SO_4 (1:2 wt ratio), the crystalline nature of the material decreases and amorphous nature of the material increases. This result was supported by Blanco et al., (2005). However, in the present case, the intensity of the acid treated metal impregnated FA is not lower than the water washed fly ash. This contrasting result in the present studies might be due to the use of lower concentration of acid with respect to FA (2.6:1 wt ratio). However, with alkali treated FA catalysts, in all the twelve cases, the intensity of the basal peak was lower than the basal peak of water washed counterparts; indicating that alkali treated FA lowers the crystalline nature of the FA materials.

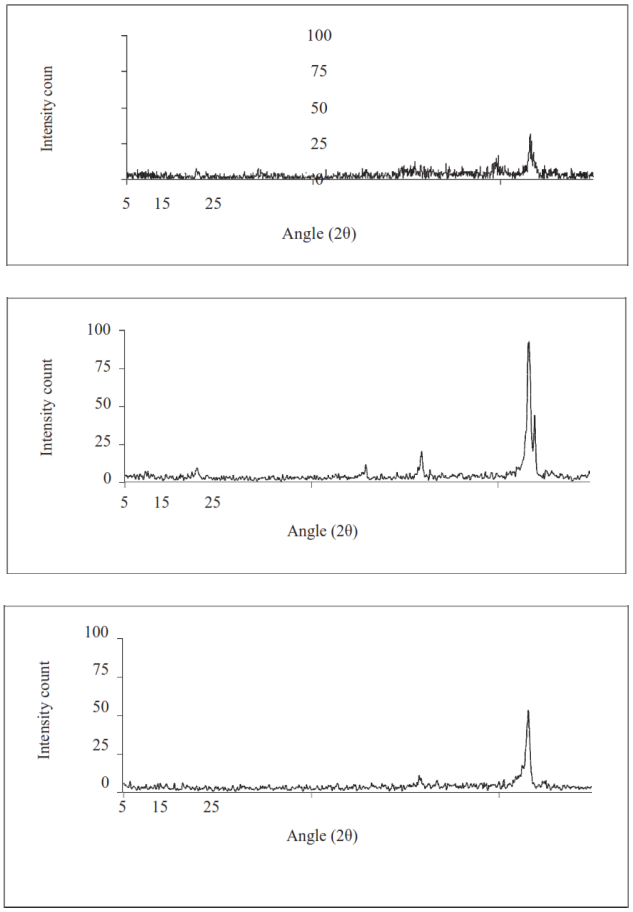

Figure. 5. XRD patterns for calcined Fe(III)-impregnated water washed (F1, top), acid treated (F2, middle) and alkali treated (F3, bottom) fly ash catalysts.

FOURIER TRANSFORMS INFRARED (FT-IR) SPECTROSCOPY

The FT-IR spectroscopy was an extensively useful method for the determination of various functional groups present in the catalysts. The FTIR measurements of the raw fly ash and the catalysts, in this work, have been interpreted as follows:

(i) Calcined raw fly ash (O)

The FT-IR spectra of calcined raw fly ash (O) are shown in Fig. 6. The assignment of all the major FT-IR bands present in the material are discussed below:

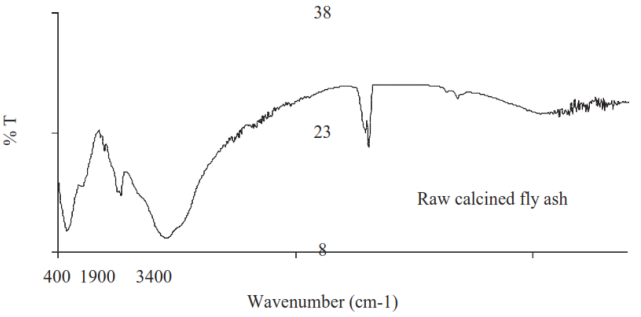

Figure. 6: FT-IR spectra of calcined raw fly ash sample (O)

(i) The material showed a prominent IR band at around 1099.4 cm^{-1} which may be attributed to the Si–O–Si asymmetric stretching. Two other bands around 798 and 470 cm^{-1} were also observed. These bands are typical for Si-O bending vibrations of quartz present in the fly ash as a major constituent. Absorption around 1103 cm^{-1} could be assigned to Fe-O vibrations arising from the considerable amount of iron present in the fly ash as Fe_2O_3 (Sarkar et al, 2006; Li et al, 2009).

(ii) The band observed between 2931 and 2862 cm^{-1} could be assigned to the asymmetric and symmetric stretching of – CH_2 groups from residual carbon compounds in the fly ash.

(iii) The broad absorption band between 3650–3400 cm^{-1} (Fig. 6) was attributed to the presence of hydrogen bond between the vicinal pairs of surface – OH groups of Si-OH and adsorbed water molecules on the surface (Sarkar et al, 2006; Li et al, 2009).

(ii) Mn(II)-impregnated fly ash

The FT-IR spectra of Mn(II)-water washed fly ash (M1), Mn(II)-acid treated fly ash (M2) and Mn(II)-alkali treated fly ash (M3) are shown in Fig. 7. The assignment of the IR bands is given in Table 8. The 1099.4 cm^{-1} band assigned to asymmetric Si-O stretching showed a little shift in the three catalysts when compared with that of the raw fly ash. Thus, the band at 1099.4 cm^{-1} shifted to

- 1083.8 cm^{-1} in Mn(II)-water washed fly ash (M1)
- 1087.8 cm^{-1} in Mn(II)-acid treated fly ash (M2)
- 1103.3 cm^{-1} in Mn(II)-alkali treated fly ash (M3).

However, such shift was not observed for Si-O bending vibrations (798 and 470 cm^{-1}) in Mn(II)-fly ash materials. Only a little change in the peak intensities was noticed.

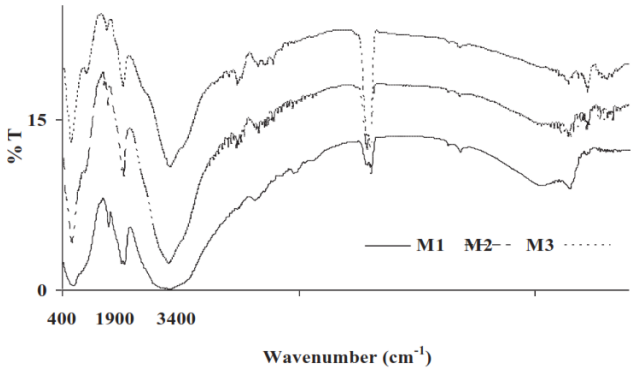

Figure. 7: FT-IR spectra of the calcined samples of Mn(II)-impregnated water washed (M1), acid treated (M2), alkali treated (M3) fly ash.

The absorption band at 2860 to 2940 cm^{-1}, assigned to the asymmetric and symmetric stretching of – CH_2 groups in the raw fly ash, was also present in the impregnated catalysts, but with reduced intensities. All the three catalysts had a OH- stretching band at 3650–3400 cm^{-1}. However, the bands observed at 1527.6, 1519.9 and 1516.0 cm^{-1} in M1, M2 and M3 respectively are assigned to O-H bending vibrations. These bands are conspicuously absent or are not clearly observed in the raw fly ash.

Table 8: IR bands (cm-1) of the calcined samples of Mn(II)-impregnated catalysts (M1, M2, M3) along with their assignment

IR bands (cm^{-1})			Assignment
M1	M2	M3	
478.3	474.5	470.6	Si-O bending
798.5	798.5	798.5	
1099.4	1103.3	1107.1	Si-O-Si asymmetric stretching
1527.6	1519.9	1516.0	O-H bending
1639.5	1654.9	1658.8	deformation vibration
2935.7	2939.5	2935.6	Aliphatic C-H stretching
3483.4	3525.8	3579.8	Hydrogen bonded Si-OH

(iii) Co(II)-impregnated fly ash

The FT-IR spectra of Co(II)-water washed fly ash (C1), Co(II)-acid treated fly ash (C2) and Co(II)-alkali treated fly ash (C3) are shown in Fig. 8. Assignment of the bands is given in Table 9.

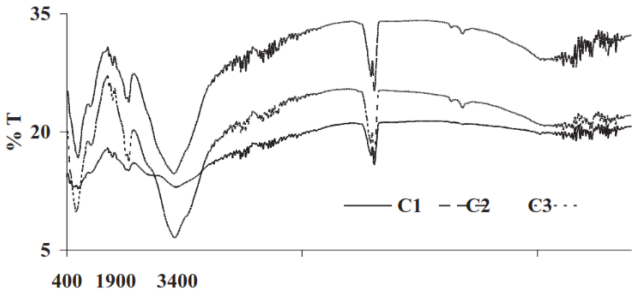

Figure. 8: FT-IR spectra for the calcined samples of Co(II)-water washed fly ash (C1), Co(II)-acid treated fly ash (C2), Co(II)-alkali treated (C3) fly ash.

Fig.8 shows that the asymmetric Si-O stretching band at 1099.4 cm-1 observed in the parent fly ash shifted to lower frequencies of 1095.6 cm-1, 1080.1 cm-1, and 1087.9 cm-1 for C1, C2 and C3 respectively. The shift was maximum in case of C2, i.e., Co(II)-acid treated fly ash. At the same time, Si-O bending frequencies around 798 and 470 cm^{-1}, observed in the raw fly ash (O), were also present in all the three Co(II) impregnated catalysts without any noticeable shift but with a little change in the peak intensity.

The small peak observed at 2924.1 cm^{-1} in the three catalysts is assigned to asymmetric and symmetric stretching of – CH_2 groups originated in the raw fly ash (O). The broad O-H stretching band at 3600 – 3450 cm^{-1} is also observed in the three catalysts. This broad appeared at 3479.5 cm^{-1} in Co(II)-water washed fly ash and was shifted to 3568.3 cm^{-1} in C2 and 3545.2 cm^{-1} in C3. However, the bands observed at 1523.8, 1523.7 and 1508.3 for C1, C2 and C3 respectively and typically assigned to O- H bending vibrations were not clearly observed in the raw fly ash.

(iv) Ni(II)-impregnated fly ash

FT-IR spectra of Ni(II)-water washed fly ash (N1), Ni(II)-acid treated fly ash (N2) and Ni(II)-alkali treated fly ash (N3) are shown in Fig. 9. The assignment of the bands is given in Table 10.

As in the case of Mn(II)-fly ash and Ni(II)-fly ash, the band assigned to asymmetric Si-O stretching was shifted to a lower frequency in comparison to the band at 1099.4 cm^{-1} obtained for the raw fly ash. This band now appeared at 1091.7 cm^{-1}, 1083.9 cm^{-1}, and 1087.9 cm^{-1} respectively for N1, N2 and N3.

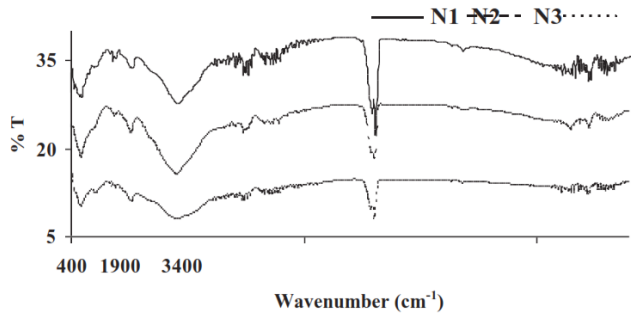

Fig. 9: FT-IR spectra of the calcined samples of Ni(II)-impregnated water washed (N1), acid treated (N2), alkali treated (N3) fly ash.

Table 9: IR bands (cm-1) of the calcined samples of Co(II)-fly ash (C1, C2, C3) along with their assignment

IR bands (cm^{-1})			
C1	C2	C3	Assignment
470.6	474.5	459.1	Si-O bending
798.7	794.7	779.2	
1095.6	1080.1	1087.9	Si-O-Si asymmetric stretching
1523.8	1523.7	1508.3	O-H bending
1654.9	1654.9	1651.1	deformation vibration
2924.1	2924.1	2924.1	Aliphatic C-H stretching
3479.5	3568.3	3545.2	Hydrogen bonded Si-OH

Table 10: IR bands (cm-1) of the calcined samples of Ni(II)-impregnated catalysts (N1, N2, N3) along with their assignment.

IR bands (cm^{-1})			
N1	N2	N3	Assignment
470.6	470.6	470.6	Si-O bending
794.7	790.8	794.7	
1091.7	1083.9	1087.9	Si-O-Si asymmetric stretching
1519.9	1512.2	1519.9	O-H bending
1651.1	1647.2	1651.1	deformation vibration
2924.1	2924.1	2924.1	Aliphatic C-H stretching
3444.9	3498.9	3502.7	Hydrogen bonded Si-OH

The bands assigned to Si-O bending around 798 and 470 cm−1 in raw fly ash (O) showed slight shift in all the three catalysts accompanied by some change in the peak intensity. The Si-O bending frequencies were observed at 470.6 and 794.7 cm-1, 470.6 and 790.8 cm-1, and 470.6 and 794.7 cm-1 respectively for Ni(II)-water washed fly ash (N1), Ni(II)-acid treated fly ash (N2) and Ni(II)-alkali treated fly ash (N3).

A small band appearing at 2860 to 2940 cm^{-1} in the Ni-fly ash catalyst is assigned to the asymmetric and symmetric stretching of – CH_2 groups originating from the raw fly ash. The catalysts also show broad IR bands at 3650–3400 cm^{-1} due to O-H stretching and bands at 1519.9, 1512.2 and 1519.9 cm^{-1} respectively in N1, N2 and N3 which could be assigned to O-H bending vibrations. It may be noted that the OH-bending vibrations were not clearly observed in the raw fly ash.

(v) Fe(III)-impregnated fly ash

The FT-IR spectra of the three Fe(III) impregnated fly ash viz. Fe(III)-water washed fly ash (F1), Fe(III)-acid treated fly ash (F2) and Fe(III)-alkali treated fly ash (F3) are shown in Fig. 10 and the assignment of the bands is given in Table 11.

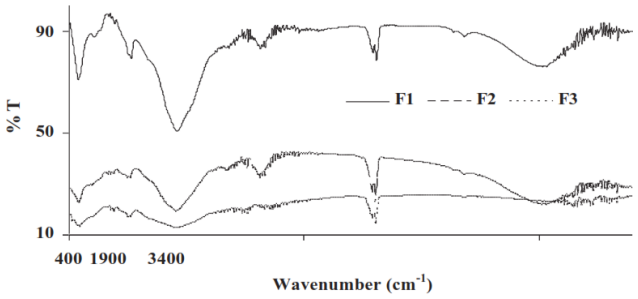

Figure. 10: FT-IR spectra of calcined samples of Fe(III)-impregnated water washed (F1), acid treated (F2), alkali treated (F3) fly ash.

Table 11: IR bands (cm-1) of the calcined samples of Fe(III)-impregnated catalysts (F1, F2, F3) along with their assignment

IR bands (cm^{-1})			
F1	F2	F3	Assignment
459.1	466.8	474.5	Si-O bending
794.7	794.7	779.2	
1087.9	1087.9	1087.9	Si-O-Si asymmetric stretching
1523.8	1508.3	1508.3	O-H bending
1624.1	1639.5	1651.1	deformation vibration
2924.1	2927.9	2924.1	Aliphatic C-H stretching
3421.7	3464.2	3444.9	Hydrogen bonded Si-OH

As in the other cases, the asymmetric Si-O stretching band was shifted from 1099.4 cm^{-1} (raw fly ash) to 1087.9 cm^{-1}, 1087.9 cm^{-1} and 1087.9 cm^{-1} respectively for Fe(III)- water washed fly ash (F1), Fe(III)-acid treated fly ash and Fe(III)-alkali treated fly ash. The shift was considerable.

The Si-O bending bands (around 798 and 470 cm^{-1} in raw fly ash) shifted to 459.1 and 794.7 cm^{-1} in F1, 466.8 and 794.7 cm^{-1} in F2, and 474.5 and 779.2 cm^{-1} in F3. The small peak in the range of 2860 to 2940 cm^{-1} assigned to asymmetric and symmetric

stretching of – CH_2 groups in the raw fly ash was also shifted towards a lower wave number. The broad IR band between 3650–3400 cm^{-1} assigned to O-H stretching was also observed in the three catalysts along with the O-H bending bands at 1523.8, 1508.3 and 1508.3 $cm^{-1}$for F1, F2 and F3 respectively. The OH bending vibrations were not prominently observed in the raw fly ash.

Lot of researchers had reported the FT-IR bands for fly ash material. Kumar et al. (2014) had reported that the broad band (around 3500 cm^{-1}) and a small peak around 1620 cm^{-1} found in the fly ash was corresponds to silanol group of the catalyst and bending O-H band water molecule. In the present work both these two bands are observed approximately in the same region.

CONCLUSION

The characterization of the materials was done with (a) Atomic adsorption spectrophotometry to find out the amount of the transition metal entering into the fly ash support, (b) X-ray fluorescence to determine to chemical composition of the catalysts,

X-ray diffraction to identify the crystallographic phases, (d) Scanning electron microscopy to get information about the surface topography, (f) BET surface area, pore volume and pore diameter and (g) Cation exchange capacity measurements.

REFERENCES

1. Alinnor, I.J., Nwachukwu, M.A. (2011). A study on removal characteristics of para- nitrophenol from aqueous solution by fly ash, Journal of Environmental Chemistry and Ecotoxicology, 3(2), pp. 32–36.

2. ASTM standard specification for coal fly ash and raw or calcined natural pozzolan for use in concrete (C618-05). (2005) In: Annual book of ASTM standards, concrete and aggregates, 04.02. American Society for Testing Materials.

3. Ayala, J., Blanco, F., Garcia, P., Rodriguez, P. Sancho, J. (1998). Asturian fly ash as a heavy metals removal material, Fuel, 77 (11), pp. 1147 – 1154.

4. Babajide, O., Petrik, L., Musyoka, N., Amigun, B., Ameer, F. (2010). Use of coal fly ash as a catalyst in the production of biodiesel, Petroleum & Coal, 52(4), pp. 261–272.

5. Catrinescu, C., Arsene, D., Teodosiu, C. (2011) Catalytic wet hydrogen peroxide oxidation of para-chlorophenol over Al/Fe pillared clays (AlFePILCs) prepared from different host clays. Applied Catalysis B: Environmental, 101, pp. 451–460.

6. Eletzke, G.H. (1966). Wet Air Oxidation - Industrial Waste Applications, 39th Annual Conference, Water Pollution Control Federation.

7. Fernández, J., Renedo, J., Garea, A., Viguri, J., Irabien, J.A. (1997). Preparation and characterization of fly ash/hydrated lime sorbents for SO_2 removal, Powder Technology, 94, pp. 133-139.

8. Gupta, S.K, Gupta, S.K., Hung, Y.T. (2006). Treatment of pharmaceutical waste, In: Wang, L.K., Hung, Y.T., Howard, H.L. and Yapijakis C. (eds.), Waste treatment in the process industries, CRC Taylor and Francis, pp. 167–233.

9. Jain, D., Mishra, M., Rani, A. (2012). Synthesis and characterization of novel aminopropylatedfly ash catalyst and its beneficial application in base catalyzed Knoevenagel condensation reaction, Fuel Processing Technology, 95, pp. 119-126.

10. Jain, K.K., Prasad, G., Sinah, V.N. (1980) Application of Langmuir isotherm for oxalic adsorption by fly ash and activated carbon. Indian Journal of Chemistry B, 19, pp. 154–6.

11. Johnson, A., Catalan, L.J.J., Kinrade, S.D. (2010). Characterization and evaluation of fly-ash from co-combustion of lignite and wood pellets for use as cement admixture, Fuel, 89, pp. 3042–3050.

12. Jovanovic, G.N., Plazl, P.Ž., Sakrittichai, P., Al-Khaldi, K. (2005) Dechlorination of p-Chlorophenol in a Microreactor with Bimetallic Pd/Fe Catalyst Industrial Engineering Chemistry Research, 44, pp. 5099-5106.

13. Manz, O.E. (1999) Coal fly ash: a retrospective and future look, Fuel, 78(2), pp. 133–6.

Corresponding Author

Sandeep Kumar*

Research Scholar, Maharishi University of Information Technology, Lucknow